Monthly Notices of the ROYAL ASTRONOMICAL SOCIETY

Mon. Not. R. Astron. Soc. **407,** 1223–1230 (2010) doi:10.1111/j.1365-2966.2010.16975.x

A Toomre-like stability criterion for the clumpy and turbulent interstellar medium

Alessandro B. Romeo,[1★] Andreas Burkert[2] and Oscar Agertz[3]

[1]*Onsala Space Observatory, Chalmers University of Technology, SE-43992 Onsala, Sweden*
[2]*University Observatory, University of Munich, Scheinerstr. 1, D-81679 Munich, Germany*
[3]*Institute for Theoretical Physics, University of Zürich, CH-8057 Zürich, Switzerland*

Accepted 2010 May 6. Received 2010 April 22; in original form 2010 January 26

ABSTRACT

We explore the gravitational instability of clumpy and turbulent gas discs, taking into account the Larson-type scaling laws observed in giant molecular clouds (GMCs) and H I, as well as more general scaling relations. This degree of freedom is of special interest in view of the coming high-z interstellar medium surveys and is thus potentially important for understanding the dynamical effects of turbulence at all epochs of galaxy evolution. Our analysis shows that turbulence has a deep impact on the gravitational instability of the disc. It excites a rich variety of stability regimes, several of which have no classical counterpart. Among other diagnostics, we provide *two useful tools* for observers and simulators: (1) the stability map of turbulence, which illustrates our stability scenario and relates it to the phenomenology of interstellar turbulence: GMC/H I observations, simulations and models; (2) a Toomre-like stability criterion, $Q \geq \overline{Q}$, which applies to a large class of clumpy/turbulent discs. We make specific predictions about GMC and cold-H I turbulence and point out the implications of our analysis for high-z galaxy surveys.

Key words: instabilities – turbulence – ISM: general – ISM: kinematics and dynamics – ISM: structure – galaxies: ISM.

1 INTRODUCTION

Toomre's (1964) stability criterion, $Q \geq 1$, is one of the pillars of disc galaxy dynamics (see e.g. Binney & Tremaine 2008). It is used in a wide variety of contexts, in star formation for example, where the gravitational instability of the interstellar gas plays a critical role (e.g. Quirk 1972; Kennicutt 1989; Martin & Kennicutt 2001; Schaye 2004, 2008; Burkert 2009; Elmegreen 2009).

So why introduce a new stability criterion? We do this because behind Toomre's criterion there is one fundamental assumption: the medium is approximately in equilibrium, with well-defined surface density Σ and velocity dispersion σ. But this is far from being true in the clumpy and turbulent interstellar gas, where such quantities depend strongly on ℓ, the size of the region over which they are measured. In fact, a fundamental aspect of interstellar turbulence is the existence of density– and velocity–size scaling laws: $\Sigma \propto \ell^a$ and $\sigma \propto \ell^b$ (see e.g. Elmegreen & Scalo 2004; McKee & Ostriker 2007). In giant molecular clouds (GMCs), the scaling exponents are $a \approx 0$ and $b \approx \frac{1}{2}$ (e.g. Larson 1981; Solomon et al. 1987; Bolatto et al. 2008; Heyer et al. 2009; Hughes et al. 2010). In the H I component, density and velocity fluctuations seem to have a Kolmogorov spectrum *up to galactic scales*: $a \sim \frac{1}{3}$ for $\ell \lesssim 10$ kpc and $b \sim \frac{1}{3}$ for $\ell \lesssim 1$ kpc (e.g. Lazarian & Pogosyan 2000; Elmegreen, Kim & Staveley-Smith 2001; Begum, Chengalur & Bhardwaj 2006; Kim et al. 2007; Dutta et al. 2008; Roy, Peedikakkandy & Chengalur 2008; Dutta et al. 2009a,b). Note, however, that the uncertainties are large, especially in the H I case. Further evidence for interstellar medium (ISM) turbulence is provided by the 'Big Power Law in the Sky', i.e. the fact that electron density fluctuations show a Kolmogorov spectrum over a wide range of scales: from 10^3 km up to 10 pc (Armstrong, Rickett & Spangler 1995; see Chepurnov & Lazarian 2010, for the most recent determination of the upper scale).

Clumpy and turbulent gas is also observed in high-redshift star-forming galaxies, where it dominates the morphology and dynamics of the disc (e.g. Wadadekar, Casertano & de Mello 2006; Elmegreen et al. 2007; Genzel et al. 2008; Shapiro et al. 2008; Förster Schreiber et al. 2009). Coming surveys will tell us how Σ and σ scale with ℓ at high z and thus how turbulence develops in disc galaxies. This is one of the hot topics in modern astrophysics (e.g. Krumholz & Burkert 2010), and several state-of-the-art simulations have already been designed for such a purpose (e.g. Wada, Meurer & Norman 2002; Kim & Ostriker 2007; Levine et al. 2008; Agertz et al. 2009a; Bournaud & Elmegreen 2009; Dekel, Sari & Ceverino 2009; Tasker & Tan 2009; Agertz, Teyssier & Moore 2009b). In order to interpret

★E-mail: romeo@chalmers.se

such data correctly, one must understand in detail how turbulence affects the (in)stability of the disc.

All of these facts together motivate a thorough investigation of the problem.

Elmegreen (1996) assumed Larson-type scaling relations, $\Sigma \propto \ell^a$ and $\sigma \propto \ell^b$, and investigated the case $a = -1$ and $b = \frac{1}{2}$. He found that the disc is always stable at large scales and unstable at small scales. To the best of our knowledge, this was the only theoretical work devoted to the gravitational instability of clumpy/turbulent discs before ours. In contrast, several investigations focused on the effects of turbulence on Jeans instability (e.g. Bonazzola et al. 1987; Just, Jacobi & Deiss 1994; Vázquez-Semadeni & Gazol 1995).

The goal of our paper is to explore the gravitational instability of clumpy/turbulent discs, spanning the whole range of values for a and b. Among other diagnostics, we provide the following two useful tools for observers and simulators.

(i) *The stability map of turbulence.* Using a and b as coordinates, we illustrate the natural variety of stability regimes possessed by such discs and populate this diagram with observations, simulations and models of interstellar turbulence (Fig. 1).

(ii) *A Toomre-like stability criterion.* We show that in our map there is a densely populated domain where the stability criterion is of the form $Q \geq \overline{Q}$, and determine the stability threshold $\overline{Q}$ as a function of a, b and of the scale at which Q is measured (equation 17 and Fig. 2). If our criterion is fulfilled, then the disc is stable at all scales [the case investigated by Elmegreen (1996) lies in another stability regime].

The rest of the paper is organized as follows. In Section 2, we determine a dispersion relation that takes fully into account the scaling laws of interstellar turbulence as well as the thickness of the gas layer. We then surf through the various stability regimes. Our Toomre-like stability criterion is given in Section 2.7, together with other important diagnostics: the most unstable scale and its growth rate. In Section 3, we discuss the stability map of turbulence. We then make specific predictions about strongly and weakly supersonic turbulence. In Section 4, we explore the densely populated Toomre-like domain and illustrate the stability diagnostics in a number of cases, taking into account the saturation of density and velocity at large scales. In Section 5, we draw the conclusions.

2 STABLE OR UNSTABLE?

2.1 The turbulent dispersion relation

Consider a gas disc of scaleheight h and perturb it with axisymmetric waves of frequency ω and wavenumber k. The response of the disc is described by the dispersion relation

$$\omega^2 = \kappa^2 - \frac{2\pi G \Sigma\, k}{1 + kh} + \sigma^2 k^2\,, \tag{1}$$

where κ is the epicyclic frequency, Σ is the surface density at equilibrium and σ is the sound speed (Romeo 1990, 1992, 1994; see also Vandervoort 1970). So the three terms on the right-hand side of equation (1) represent the contributions of rotation, self-gravity and pressure. For $kh \ll 1$, equation (1) reduces to the usual dispersion relation for an infinitesimally thin gas disc (see e.g. Binney & Tremaine 2008). For $kh \gg 1$, one recovers the case of Jeans instability with rotation, since $\Sigma/h \approx 2\rho$. In other words, scales comparable to h mark the transition from 2D to 3D stability. Note that we can encapsulate the effect of thickness in a single quantity and rewrite equation (1) as

$$\omega^2 = \kappa^2 - 2\pi G \Sigma_{\mathrm{eff}}\, k + \sigma^2 k^2\,, \tag{2}$$

where $\Sigma_{\mathrm{eff}} = \Sigma/(1 + kh)$ is the effective surface density. Σ_{eff} and σ are two important quantities, which we discuss in detail below.

(i) *The effective surface density*. What is the relation between Σ_{eff} and ρ? Since $\Sigma_{\mathrm{eff}} = \Sigma/(1 + kh)$ and $\Sigma \sim \rho h$, we find that $\Sigma_{\mathrm{eff}} \sim \rho h$ if $kh \lesssim 1$ and $\Sigma_{\mathrm{eff}} \sim \rho/k$ otherwise. This means that the observational counterpart of Σ_{eff} is the mass column density measured over a region of size $\ell = 1/k$. In the cold ISM, which is highly supersonic and hence strongly compressible, the amplitude of density fluctuations is typically much larger than the mean density. Density fluctuations have a power-law energy spectrum, $E_\rho(k) \propto k^{-r}$, which means $\rho \propto k^{-(r-1)/2}$ (see e.g. Elmegreen & Scalo 2004). A power-law spectrum is then imprinted on Σ_{eff}:

$$\Sigma_{\mathrm{eff}} = \Sigma_0 \left(\frac{k}{k_0}\right)^{-a}. \tag{3}$$

Using the relation between Σ_{eff} and ρ that we have found above, we can relate a to r: $a = \frac{1}{2}(r-1)$ for $kh \lesssim 1$, while $a = \frac{1}{2}(r+1)$ for $kh \gtrsim 1$. In the warm ISM, which is transonic or subsonic and hence weakly compressible, the density contrast is typically small so Σ_{eff} is dominated by the mean density, as in the limiting case of a non-turbulent disc: $\Sigma_{\mathrm{eff}} =$ constant for small k, while $\Sigma_{\mathrm{eff}} \propto k^{-1}$ for large k. Hereafter we will omit the subscript 'eff', unless otherwise stated.

(ii) *The sound speed*. The observational counterpart of σ is the 1D velocity dispersion measured over a region of size $\ell = 1/k$: $\sigma^2 = \sigma_{\mathrm{ther}}^2 + \sigma_{\mathrm{tur}}^2\,(k)$, where σ_{ther} and σ_{tur} are the thermal and turbulent 1D velocity dispersions, respectively. Velocity fluctuations have a power-law energy spectrum, $E_{\mathrm{v}}(k) \propto k^{-s}$, which means $\sigma_{\mathrm{tur}} \propto k^{-(s-1)/2}$ (see e.g. Elmegreen & Scalo 2004). Both thermal and turbulent motions tend to support the gas against gravitational instability. However, as pointed out by the referee, turbulent support results in relations that are true only in a statistical sense, with individual clouds collapsing even when the statistical criterion for stability is well satisfied. In the cold ISM, σ has a power-law dependence on k since it is dominated by $\sigma_{\mathrm{tur}}(k)$:

$$\sigma = \sigma_0 \left(\frac{k}{k_0}\right)^{-b}, \tag{4}$$

where $b = \frac{1}{2}(s-1)$ and s is the velocity spectral index. In the warm ISM, $\sigma(k)$ deviates significantly from a power law since σ_{ther} is no longer negligible.

Hereafter we will only consider the *cold* ISM (H_2 and cold H I), since in such a case we can explicitly take into account the power-law scaling of interstellar turbulence via equations (3) and (4). We will regard the quantity $\ell_0 = 1/k_0$ introduced in those equations as the fiducial scale at which the mass column density and the 1D velocity dispersion are observed. This is also the scale at which Q and other stability quantities are measured. Substituting equations (3) and (4) into equation (2), we obtain the final dispersion relation:

$$\omega^2 = \kappa^2 - 2\pi G \Sigma_0 k_0^a\, k^{1-a} + \sigma_0^2 k_0^{2b}\, k^{2(1-b)}\,. \tag{5}$$

Our phenomenological approach differs significantly from the traditional way to include turbulent effects in the dispersion relation, which is to identify σ with the typical 1D velocity dispersion observed at galactic scales. Bonazzola et al. (1987), Just et al. (1994), Vázquez-Semadeni & Gazol (1995) and Elmegreen (1996) adopted an approach similar to ours for investigating the gravitational instability of clumpy/turbulent media.

Equation (5) is the starting point of our stability analysis. As in the usual case, stability at all scales requires that $\omega^2 \geq 0$ for all k.[1] Whether this requirement can be satisfied or not depends on the self-gravity and pressure terms, which now scale as k^A and k^B:

$$A = 1 - a, \tag{6}$$

$$B = 2\,(1 - b)\,. \tag{7}$$

In the following, we explore all the various cases.

2.2 Case $a = 1,\ b \neq 1$

Here the self-gravity term is independent of k ($A = 0$), like the rotation term:

$$\omega^2 = \underbrace{\kappa^2 - 2\pi G\Sigma_0 k_0}_{C} + \sigma_0^2 k_0^{2b}\, k^{2(1-b)}\,. \tag{8}$$

For $b < 1$, ω^2 increases with k and tends to C as $k \to 0$. Hence, the sign of C determines whether the disc is stable at all scales or not. Stability requires that $C \geq 0$. For $b > 1$, ω^2 decreases with k and tends to C as $k \to \infty$. So, again, stability requires that $C \geq 0$. The stability criterion is then

$$\text{STABLE } \forall k \iff k_0 \leq k_\mathrm{T} = \frac{\kappa^2}{2\pi G\Sigma_0}\,. \tag{9}$$

Equation (9) resembles Toomre's stability criterion for cold discs, $k \leq k_\mathrm{T}$, but there is one important difference: equation (9) is a condition that must be fulfilled by k_0 to ensure stability for all k, whereas the cold Toomre criterion ensures stability for small k.

2.3 Case $a \neq 1,\ b = \frac{1}{2}(1 + a)$

Here the pressure term has the same k dependence as the self-gravity term ($B = A$):

$$\omega^2 = \kappa^2 + \underbrace{\left(\sigma_0^2 k_0^{1+a} - 2\pi G\Sigma_0 k_0^a\right)}_{C}\, k^{1-a}\,. \tag{10}$$

If $a < 1$, then ω^2 converges to κ^2 as $k \to 0$ and the sign of $\mathrm{d}\omega^2/\mathrm{d}k$ is equal to the sign of C (for $C < 0$, ω^2 diverges as $k \to \infty$). Hence, stability requires that $C \geq 0$. If $a > 1$, then ω^2 converges to κ^2 as $k \to \infty$ and the sign of $\mathrm{d}\omega^2/\mathrm{d}k$ is opposite to the sign of C (for $C < 0$, ω^2 diverges as $k \to 0$). So, again, stability requires that $C \geq 0$. The stability criterion is then

$$\text{STABLE } \forall k \iff k_0 \geq k_\mathrm{J} = \frac{2\pi G\Sigma_0}{\sigma_0^2}\,. \tag{11}$$

The resemblance between equation (11) and the 2D Jeans criterion, $k \geq k_\mathrm{J}$, is superficial. In fact, equation (11) ensures that the disc is stable at all, rather than small, scales. An analogous fact was noted in the context of our first stability criterion (equation 9).

[1] The dispersion relation assumes that $kR \gg 1$, where R is the radial coordinate (see e.g. Binney & Tremaine 2008). This local condition is more restrictive than the natural requirement $k \gtrsim 2\pi/L$, where L is the size of the gas disc. Since the above condition cannot be rigorously included in the stability analysis, the usual procedure is to consider all k and to check a posteriori whether $kR \gg 1$ or not.

2.4 Case $a = 1,\ b = 1$

Although this case seems the intersection of cases 2.2 and 2.3, the stability criterion is not $k_\mathrm{J} \leq k_0 \leq k_\mathrm{T}$. In fact, this case is singular. The self-gravity and pressure terms are independent of k ($A = B = 0$), like the rotation term, so $\omega^2(k)$ is constant:

$$\omega^2 = \underbrace{\kappa^2 - 2\pi G\Sigma_0 k_0 + \sigma_0^2 k_0^2}_{C}\,. \tag{12}$$

As C is quadratic in k_0, the inequality $C \geq 0$ can be easily solved and the resulting stability criterion is

$$\text{STABLE } \forall k \iff \begin{cases} k_0 \leq k_- \text{ or } k_0 \geq k_+ & \text{if } Q < 1\,, \\ 0 < k_0 < \infty & \text{else}\,. \end{cases} \tag{13}$$

Here k_- and k_+ are related to the Toomre wavenumber k_T (and to the Jeans wavenumber $k_\mathrm{J} = k_\mathrm{T}\, 4/Q^2$):

$$k_\pm = k_\mathrm{T}\, \frac{2}{Q^2}\left(1 \pm \sqrt{1 - Q^2}\right), \tag{14}$$

and Q is the Toomre parameter:

$$Q = \frac{\kappa\sigma_0}{\pi G\Sigma_0}\,. \tag{15}$$

The $Q < 1$ case of equation (13) resembles the corresponding Toomre stability condition, but see the remarks following equations (9) and (11). In contrast, the $Q \geq 1$ case is identical to Toomre's criterion.

2.5 Case $a < 1,\ b > \frac{1}{2}(1 + a)$

Now $A > 0$ and $B < A$. Hence, the self-gravity term gets dominant for large k and makes ω^2 negative. For small k, ω^2 is positive since it is dominated by the pressure term ($B < 0$) and/or the rotation term ($B \geq 0$). As the zero(s) of $\omega^2(k)$ can only be determined numerically, case by case, we do not give a stability criterion but note that the disc is *unstable at small scales*, like a cold non-turbulent disc.

2.6 Case $a > 1,\ b < \frac{1}{2}(1 + a)$

In contrast to the previous case, $A < 0$ and $B > A$. So ω^2 is dominated by the self-gravity term and is negative for small k, while it is dominated by the pressure/rotation term and is positive for large k. Thus the disc is *unstable at large scales*, like a non-rotating non-turbulent sheet.

2.7 Case $a < 1,\ b < \frac{1}{2}(1 + a)$

When $0 < A < B$, the response of the disc is driven by pressure at small scales and by rotation at large scales, while self-gravity acts more strongly at intermediate scales. Therefore, this is a Toomre-like case: $\omega^2(k)$ has a minimum, which determines whether the disc is stable or not. More precisely, the minimum of $\omega^2(k)$ provides three useful pieces of information: the stability threshold, the most unstable scale and its growth rate. Such quantities are introduced below, while illustrative cases are discussed in Section 4.

The stability threshold $\overline{Q}$ is the value of Q above which the disc is stable at all scales:

$$\text{STABLE } \forall k \iff Q \geq \overline{Q}\,. \tag{16}$$

$\overline{Q}$ can be determined by imposing that the minimum of $\omega^2(k)$ vanishes. Even though the calculations are very lengthy, the formula is simple, especially if expressed in terms of the 'right' parameters:

$$\overline{Q} = 2\left[A^A B^{-B}(B-A)^{B-A}\left(\frac{\ell_0}{\ell_\mathrm{T}}\right)^{2A-B}\right]^{1/(2A)}, \tag{17}$$

where $\ell_\mathrm{T} = 1/k_\mathrm{T}$ is the Toomre scale. Equation (16), with $\overline{Q}$ specified by equation (17), is our stability criterion. It reduces to Toomre's criterion $Q \geq 1$ in the limiting case of a non-turbulent disc: $A = 1$, $B = 2$ $(a = b = 0)$.

The most unstable scale, $\ell_\mathrm{min} = 1/k_\mathrm{min}$, is given by the formula

$$\frac{\ell_\mathrm{min}}{\ell_\mathrm{T}} = \overline{\mathcal{L}}\left(Q/\overline{Q}\right)^{2/(B-A)}, \tag{18}$$

where $Q/\overline{Q}$ measures the stability level of the disc (like Q in Toomre's case) and $\overline{\mathcal{L}}$ is the value of $\ell_\mathrm{min}/\ell_\mathrm{T}$ at the stability threshold $(Q/\overline{Q} = 1)$:

$$\overline{\mathcal{L}} = \left[\frac{B-A}{B}\left(\frac{\ell_0}{\ell_\mathrm{T}}\right)^{A-1}\right]^{1/A}. \tag{19}$$

Equation (18) reduces to $\ell_\mathrm{min}/\ell_\mathrm{T} = \frac{1}{2}\,Q^2$ in Toomre's case.

The growth rate of the most unstable scale, $\gamma_\mathrm{min} = (-\omega^2_\mathrm{min})^{1/2}$, is given by the formula

$$\frac{\omega^2_\mathrm{min}}{\kappa^2} = 1 - \left(Q/\overline{Q}\right)^{-2A/(B-A)}, \tag{20}$$

which vanishes at the stability threshold. Equation (20) reduces to $\omega^2_\mathrm{min}/\kappa^2 = 1 - Q^{-2}$ in Toomre's case.

2.8 Case $a > 1,\ b > \frac{1}{2}(1 + a)$

Even $B < A < 0$ is a Toomre-like case. In fact, although the scales at which pressure and rotation dominate are reversed, self-gravity still controls intermediate scales and $\omega^2(k)$ has a minimum, which determines whether the disc is stable or not. This means that, even now, the stability criterion is

$$\text{STABLE}\ \forall k \iff Q \geq \overline{Q}. \tag{21}$$

The stability threshold $\overline{Q}$, the most unstable scale and its growth rate, ℓ_min and γ_min, are given by the same formulae as in equations (17)–(20).

3 THE STABILITY MAP OF TURBULENCE

The results of Section 2 are summarized in Fig. 1. The (a, b) plane is divided into four regions, where stability à la Toomre alternates with instability at small or large scales. The two shaded lines that separate these regions, and the point at which these lines intersect, represent transitions between different stability phases. Thus, the corresponding stability criteria are hybrid (see Sections 2.2–2.4). The points $(a, b) = (0, 0)$ and $(a, b) = (-1, \frac{1}{2})$ represent the limiting case of a non-turbulent disc and the case investigated by Elmegreen (1996). To the best of our knowledge, this was the only theoretical work devoted to the gravitational instability of clumpy/turbulent discs before ours. Fig. 1 also illustrates the most interesting stability regimes populated by models, simulations and observations of astrophysical turbulence. Such points are discussed throughout the rest of this section. Specific predictions about strongly and weakly supersonic turbulence are then made in Section 3.1.

The mass–size scaling relation, $M \propto \Sigma\ell^2 \propto \ell^{a+2}$, tells us the natural bounds of a. In fact, $D = a + 2$ is the fractal dimension of the mass distribution, which ranges from 0 to 3, so we have $-2 \leq a \leq 1$. Note that the upper bound corresponds to the case in which the destabilizing effect of self-gravity is scale-independent, i.e. to the vertical shaded line introduced above.

Does even the other shaded line have a two-fold meaning? Yes, and an important one! If the stabilizing effect of pressure has the same scale dependence as the effect of self-gravity, $b = \frac{1}{2}(1 + a)$, then $\sigma^2 \propto \ell\Sigma \propto M/\ell$, which is the virial scaling relation. GMCs are then expected to clump along that line, i.e. to populate the transition regime between stability à la Toomre and instability at small scales. For example, the well-known scaling laws Σ = constant and $\sigma \propto \ell^{1/2}$ (Larson 1981; Solomon et al. 1987) correspond to the point $(a, b) = (0, \frac{1}{2})$. Both Galactic and extragalactic GMCs show non-negligible dispersion around that point, especially along the virial line, as can be inferred from Bolatto et al. (2008) and Heyer et al. (2009). The case of perturbed galactic environments seems different. Rosolowsky & Blitz (2005) investigated the physical properties of GMCs in M64 (NGC 4826), an interacting molecule-rich galaxy, and found $\Sigma \propto M^{0.7\pm0.2}$ and $\sigma \propto \ell^{1.0\pm0.3}$, which means $(a, b) = (5^{+13}_{-3}, 1.0 \pm 0.3)$. If such scaling relations apply to individual GMCs, as was originally suggested, then each cloud is far from being in simple virial equilibrium. Besides, since (a, b) is below the virial line and on the right of the $a = 1$ line, the H_2 disc is unstable at large scales (in the sense specified in Section 2.6) and the fractal dimension is formally higher than 3. Alternatively, one may argue that these scaling relations arise from the superposition of more GMCs, each characterized by the standard scaling laws, but with proportionality factors varying significantly over the disc (Rosolowsky, private communication).

Now what about H I? A turbulence model that is becoming more and more popular is the one introduced by Fleck (1996), which predicts $\rho^{1/3}\sigma \propto \ell^{1/3}$. To understand the meaning of this scaling relation, compare it with Kolmogorov's law $\sigma \propto \ell^{1/3}$. Fleck's relation tells us that in a turbulent medium with both velocity and density fluctuations, the quantity $\rho^{1/3}\sigma$ plays a role similar to σ in incompressible turbulence. Fleck (1996) assumed that $\Sigma \sim \rho\ell$, which means $\ell \lesssim h$ (see Section 2.1). So his prediction corresponds to the line $b = \frac{1}{3}(2 - a)$, which crosses several stability regimes. The limiting case of Kolmogorov turbulence, $(a, b) = (1, \frac{1}{3})$, lies in the transition regime between stability à la Toomre and instability at large scales. Both high-resolution simulations of supersonic turbulence and H I observations populate the Toomre-like domain. Such simulations cluster along the Fleck line, near $(a, b) = (\frac{1}{2}, \frac{1}{2})$, the case of Burgers turbulence (Kowal & Lazarian 2007; Kritsuk et al. 2007; Schmidt, Federrath & Klessen 2008; Price & Federrath 2010; see also Fleck 1996, and references therein). In weakly supersonic regimes, simulations cluster closer to the Kolmogorov limit $(a, b) = (1, \frac{1}{3})$, as we will show in Section 3.1. Observed H I intensity fluctuations, which are primarily due to *cold*[2] H I (Lazarian & Pogosyan 2000), show large scatter around $(a, b) = (\frac{1}{3}, \frac{1}{3})$, i.e. they suggest a Kolmogorov scaling for both velocity and density fluctuations (e.g. Lazarian & Pogosyan 2000; Elmegreen et al. 2001; Begum et al. 2006; Dutta et al. 2008, 2009a,b). Such a scaling is also consistent with other H I observations (e.g. Kim et al. 2007; Roy et al. 2008). The simulations by Agertz et al. (2009a), designed to explore the development of H I turbulence in disc galaxies, suggest power-law indices consistent with the observed ones, except before the fragmentation of the disc (Agertz et al., in preparation).

Note that there is a very interesting and unexpected case where Fleck's model fits the observations well: the transition from H I

[2] Hereafter we will omit 'cold' when referring to H I, since our analysis also focuses on the cold ISM (see Section 2.1).

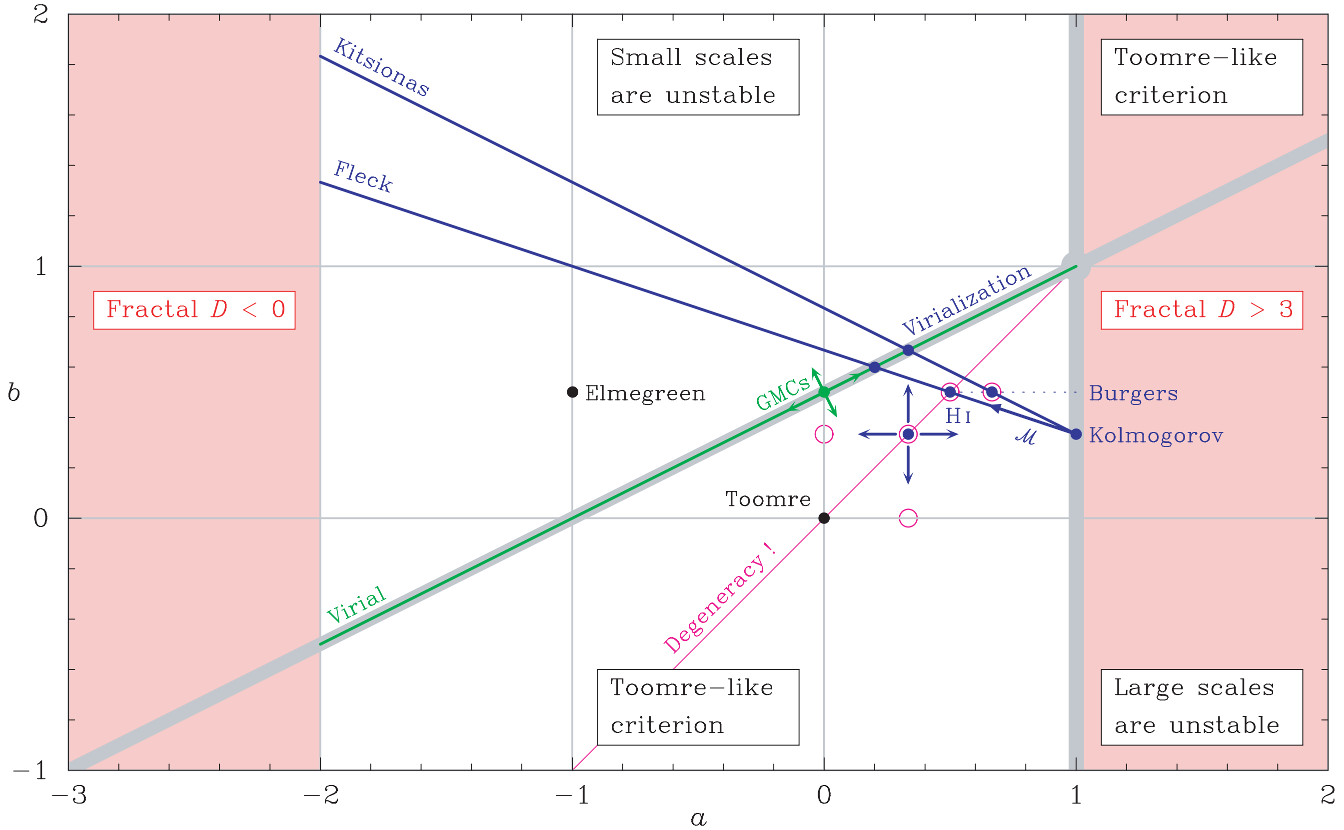

Figure 1. The stability map of turbulence. The coordinates a and b are the exponents of the density– and velocity–size scaling relations (see equations 3 and 4). The shaded lines, their intersection point and the regions between them represent the variety of stability regimes possessed by clumpy/turbulent discs. The points $(a, b) = (0, 0)$ and $(a, b) = (-1, \frac{1}{2})$ correspond to the limiting case of a non-turbulent disc and to the case investigated by Elmegreen (1996). The non-shaded part of the plane shows the natural range of a. The thick lines are phenomenological models of GMC and H I turbulence, the semiclosed-head arrows represent observations, while the closed-head arrow represents simulations with increasing Mach number. The solid circles correspond to points of special interest in astrophysical turbulence. Also shown are the cases illustrated in Figs 2 and 3 (hollow circles) and the degeneracy condition discussed in Section 4 (thin line). Note that the stability criterion is $Q \geq 1$ along such a line.

to GMC turbulence. Clumps that climb up the Fleck line become progressively more self-gravitating and will virialize at $(a, b) = (\frac{1}{5}, \frac{3}{5})$. This is close to $(a, b) = (0, \frac{1}{2})$, the reference point for GMC observations. The predicted energy spectra are $E_\Sigma(k) \propto \mathrm{d}\Sigma^2/\mathrm{d}k \propto k^{-7/5}$ and $E_\sigma(k) \propto \mathrm{d}\sigma^2/\mathrm{d}k \propto k^{-11/5}$ (the Kolmogorov spectrum scales as $k^{-5/3}$).

Low-resolution simulations of supersonic turbulence suggest an alternative scaling relation: $\rho^{1/2}\sigma \propto \ell^{1/3}$ (Kitsionas et al. 2009). In comparison with the Fleck case, this scaling gives more weight to density fluctuations and translates into a steeper line: $b = \frac{1}{2}(\frac{5}{3} - a)$, where it is again assumed that $\Sigma \sim \rho\ell$. The cases of Kolmogorov and Burgers turbulence correspond to $(a, b) = (1, \frac{1}{3})$ and $(a, b) = (\frac{2}{3}, \frac{1}{2})$, while the virialization point is $(a, b) = (\frac{1}{3}, \frac{2}{3})$. The Kitsionas line crosses the same stability regimes as the Fleck line, but lies farther away from H I and GMC observations.

3.1 Strongly versus weakly supersonic turbulence

Although our analysis focuses on strongly supersonic turbulence (see Section 2.1), here we extend it to weakly supersonic regimes (the case of a transonic or subsonic medium was considered in Section 2.1).

How does the Mach number affect the density– and velocity–size scaling relations? And how does it affect the stability of the disc? To answer these questions, one should not compute a and b directly from the density and velocity spectral indices. One should first evaluate the typical density contrast of the medium (see Section 2.1). The density probability distribution is approximately lognormal, and its mean μ and standard deviation (SD) depend on the rms Mach number $\mathcal{M}$ (Padoan, Jones & Nordlund 1997): $\mu = \frac{1}{2}\mathrm{SD}^2 \approx \frac{1}{2}\ln(1 + \frac{1}{4}\mathcal{M}^2)$. For such a distribution, the mass-weighted median density is $\rho_{\mathrm{med}} = \bar{\rho}\mathrm{e}^{\mu} \approx \bar{\rho}\,(1 + \frac{1}{4}\mathcal{M}^2)^{1/2}$, where $\bar{\rho}$ is the mean density (see section 2.1.4 of McKee & Ostriker 2007). This provides a robust estimate of the typical density (mean plus fluctuations) in the medium. The corresponding density contrast is $\delta_{\mathrm{med}} = (\rho_{\mathrm{med}} - \bar{\rho})/\bar{\rho}$.

In weakly supersonic turbulence ($\mathcal{M} \approx 2$), we have $\delta_{\mathrm{med}} \approx 0.4$ so the mass column density at scale ℓ is dominated by the mean density: $\Sigma_{\mathrm{eff}} \approx \bar{\rho}\ell$ (hence $a \approx 1$) for $\ell \lesssim h$, while $\Sigma_{\mathrm{eff}} \approx \bar{\rho}h$ (hence $a \approx 0$) for $\ell \gtrsim h$. In contrast, the 1D velocity dispersion at scale ℓ is dominated by the turbulent term: $\sigma \approx \sigma_{\mathrm{tur}}(\ell) \propto \ell^b$. For $\ell \lesssim h$, we can relate b to a using Fleck's model, $b = \frac{1}{3}(2 - a)$, and get $(a, b) \approx (1, \frac{1}{3})$. *Thus,* weakly supersonic 3D turbulence drives the disc to the boundary of the Toomre-like domain, near the Kolmogorov point.

In strongly supersonic turbulence ($\mathcal{M} \gtrsim 5$), we have $\delta_{\mathrm{med}} \gtrsim 2$ so both the mass column density and the 1D velocity dispersion are dominated by turbulent fluctuations. We can then compute a and

b from the density and velocity spectral indices (see Section 2.1). Simulations show that in an isothermal medium with negligible self-gravity, with or without magnetic fields, the density spectrum flattens (Beresnyak, Lazarian & Cho 2005; Kim & Ryu 2005; Kowal, Lazarian & Beresnyak 2007) and the velocity spectrum steepens (e.g. Kowal & Lazarian 2007; Kritsuk et al. 2007; Price & Federrath 2010) as the Mach number increases. At Mach 7, we find $(a, b) \sim (0.8, 0.4)$ from Kowal et al. (2007) and $(a, b) \sim (0.3, 0.6)$ from Kowal & Lazarian (2007), using Fleck's model in both cases.[3] In spite of the large uncertainties, it is clear that these points are on the left of $(1, \frac{1}{3})$ and, on average, closer to $(\frac{1}{2}, \frac{1}{2})$. *Thus* strongly supersonic 3D turbulence drives the disc well inside the Toomre-like domain, near the Burgers point.

4 ILLUSTRATIVE CASES

Let us now illustrate the stability characteristics of clumpy/turbulent discs in a number of cases, those marked with hollow circles in the Toomre-like domain of our map (see Fig. 1). The points $(\frac{1}{3}, \frac{1}{3})$, $(\frac{1}{2}, \frac{1}{2})$ and $(\frac{2}{3}, \frac{1}{2})$ are typical values of (a, b) inferred from H I observations, high- and low-resolution simulations of supersonic turbulence. The points $(\frac{1}{3}, 0)$ and $(0, \frac{1}{3})$ are the contributions of density and velocity fluctuations to the observed $(a, b) = (\frac{1}{3}, \frac{1}{3})$. For each case, we proceed in two ways. First, we assume that the density– and velocity–size scaling relations are perfect power laws, as given by equations (3) and (4), so that $\ell_0 = 1/k_0$ is the fiducial scale at which density and velocity are observed. We then evaluate the stability characteristics analytically using equations (17)–(20). Secondly, we consider more realistic scaling relations, which take into account the saturation of density and velocity at large scales:

$$\Sigma_{\rm eff} = \Sigma_0\,\mathcal{D}_\ell\,, \qquad \mathcal{D}_\ell = \begin{cases} (\ell/\ell_0)^a & \text{if } \ell \le \ell_0\,, \\ 1 & \text{else}\,; \end{cases} \tag{22}$$

$$\sigma = \sigma_0\,\mathcal{V}_\ell\,, \qquad \mathcal{V}_\ell = \begin{cases} (\ell/\ell_0)^b & \text{if } \ell \le \ell_0\,, \\ 1 & \text{else}\,; \end{cases} \tag{23}$$

where ℓ_0 is now the typical saturation scale. We then evaluate the stability characteristics numerically using the dispersion relation, equation (2), which we rewrite as

$$\frac{\omega^2}{\kappa^2} = 1 - \frac{\mathcal{D}_\ell}{(\ell/\ell_{\rm T})} + \frac{Q^2}{4}\,\frac{\mathcal{V}_\ell^2}{(\ell/\ell_{\rm T})^2}\,, \tag{24}$$

where $Q = \kappa\sigma_0/\pi G\Sigma_0$ is the Toomre parameter and $\ell_{\rm T} = 2\pi G\Sigma_0/\kappa^2$ is the Toomre scale.

Fig. 2 shows the stability threshold $\overline{Q}$, i.e. the value of Q above which the disc is stable at all scales. The first curious result is that such a diagnostic is highly degenerate. For example, look at the cases $(a, b) = (\frac{1}{3}, \frac{1}{3})$ and $(a, b) = (\frac{1}{2}, \frac{1}{2})$, which represent H I observations and high-resolution simulations of supersonic turbulence. They have $\overline{Q} \equiv 1$! Why do such cases degenerate into Toomre's case? Why does not turbulence show up? Equation (17) gives us the answer: because the effects of density and velocity fluctuations cancel out when $2A - B = 0$, i.e. along the line $b = a$ (see the map). The cases $(a, b) = (\frac{1}{3}, 0)$ and $(a, b) = (0, \frac{1}{3})$ allow us to disentangle such effects. Density fluctuations that saturate at a typical scale ℓ_0 tend to stabilize the disc by decreasing the stability threshold: $\overline{Q} < 1$ if $\ell_0 \gtrsim \frac{1}{2}\ell_{\rm T}$ and $\overline{Q} = 1$ otherwise. To understand this result, remember that such fluctuations reduce the self-gravity term in the dispersion relation by a factor $\mathcal{D}_\ell$ (see equations 22 and 24) and that self-gravity is destabilizing. Velocity fluctuations have an antagonistic effect. They reduce pressure by a factor $\mathcal{V}_\ell^2$ (see equations 23 and 24) and tend to destabilize the disc by increasing the stability threshold: $\overline{Q} > 1$ if $\ell_0 \gtrsim \frac{1}{2}\ell_{\rm T}$ and $\overline{Q} = 1$ otherwise. When density/velocity fluctuations do not saturate, their effect becomes destabilizing/stabilizing if the fiducial scale is small.

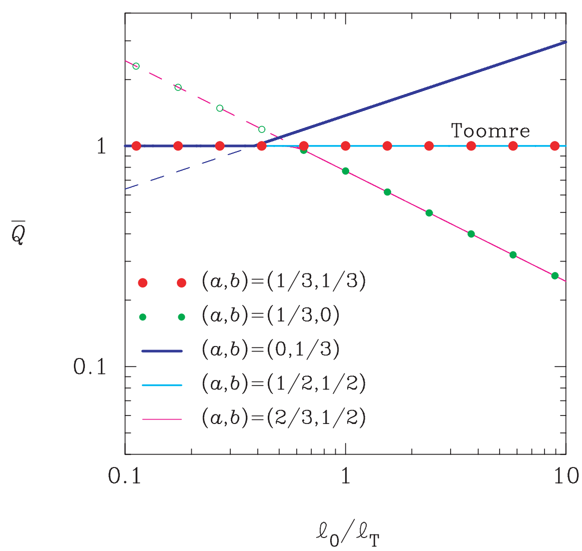

Figure 2. The stability threshold of clumpy/turbulent discs, $\overline{Q} = \overline{Q}(a, b, \ell_0)$, where a and b are the exponents of the density– and velocity–size scaling relations and ℓ_0 is the typical scale at which density and velocity saturate. In addition, $\ell_{\rm T}$ is the Toomre scale. The dashed lines and the hollow circles show the power-law behaviour predicted by equation (17) when density and velocity do not saturate; ℓ_0 is then the fiducial scale at which these quantities are observed. The limiting case of a non-turbulent disc is $\overline{Q} = 1$.

Fig. 3 shows the most unstable scale, $\ell_{\rm min}$, for two values of $Q/\overline{Q}$. Remember that this quantity measures the stability level of the disc, like Q in Toomre's case. So $Q/\overline{Q} = 1$ (top panel) means that the disc is marginally unstable, while $Q/\overline{Q} = 0.7$ (bottom panel) means that the disc is moderately unstable. In contrast to $\overline{Q}$, $\ell_{\rm min}$ is not degenerate. Turbulence now has a significant effect in the case of H I observations, since the contributions of density and velocity fluctuations are no longer antagonistic. For $\ell_0 \sim \ell_{\rm T}$, $\ell_{\rm min}$ is about 30–50 per cent smaller than in Toomre's case, depending on the value of $Q/\overline{Q}$. The impact of turbulence is stronger in the case of high-resolution simulations: the most unstable scale is typically half an order of magnitude below the expected value. Turbulent effects become less important at low resolution.

The growth rate of the most unstable scale, $\gamma_{\rm min}$, is independent of ℓ_0 and vanishes for $Q/\overline{Q} = 1$ (see equation 20). For $Q/\overline{Q} < 1$, the effects of density and velocity fluctuations cancel out when $A/(B - A) = 1$, i.e. $b = a$. This degeneracy condition is the same as that found for $\overline{Q}$ and has the same consequences.

[3] In the first case, $\mathrm{d}\ln E_\rho/\mathrm{d}\ln k$ (i.e. $-r$) is given in table 2 of Kowal et al. (2007), a is computed from r as in Section 2.1 ($\ell \lesssim h$): $a = \frac{1}{2}(r + 1)$ and b is computed from a using Fleck's model: $b = \frac{1}{3}(2 - a)$. This yields $(a, b) = (0.75 \pm 0.05, 0.42 \pm 0.02)$ for the sub-Alfvénic simulation and $(a, b) = (0.80 \pm 0.10, 0.40 \pm 0.03)$ for the super-Alfvénic simulation. In the second case (of the main text), $\mathrm{d}\ln E_v/\mathrm{d}\ln k$ (i.e. $-s$) is given in fig. 1 of Kowal & Lazarian (2007), b is computed from s as in Section 2.1: $b = \frac{1}{2}(s - 1)$ and a is computed from b using Fleck's model: $a = 2 - 3b$. This yields $(a, b) = (0.29 \pm 0.08, 0.57 \pm 0.03)$. This simulation is sub-Alfvénic, like the first one above.

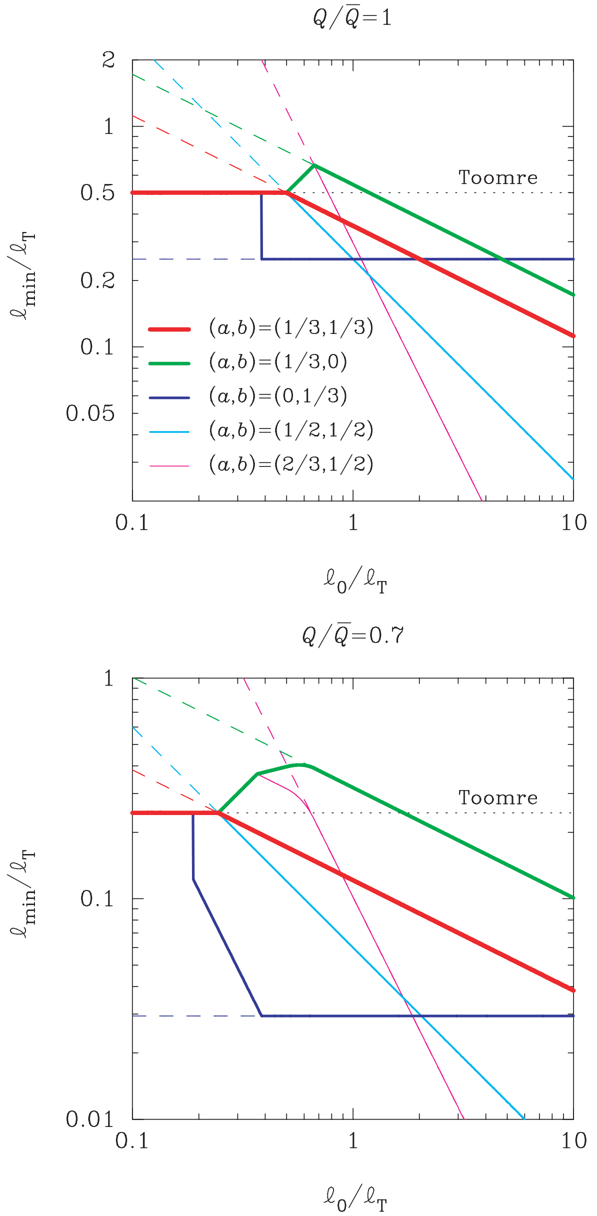

Figure 3. The most unstable scale of clumpy/turbulent discs, $\ell_{\mathrm{min}} = \ell_{\mathrm{min}}(a, b, \ell_0, Q/\overline{Q})$, where a and b are the exponents of the density– and velocity–size scaling relations, ℓ_0 is the typical scale at which density and velocity saturate and $Q/\overline{Q}$ is the stability level. In addition, ℓ_{T} is the Toomre scale. The dashed lines show the power-law behaviour predicted by equations (18) and (19) when density and velocity do not saturate; ℓ_0 is then the fiducial scale at which these quantities are observed. Also shown is the limiting case of a non-turbulent disc (dotted line).

5 CONCLUSIONS

(i) Observations and simulations of the ISM are revealing its turbulent nature with higher and higher fidelity. Such information must then be taken into account when analysing the stability of galactic discs. Our contribution is a natural extension to Toomre's work, which will prove useful for both low- and high-redshift analyses.

(ii) Turbulence has a deep impact on the gravitational instability of the disc. It excites a rich variety of stability regimes, several of which have no classical counterpart. We illustrate this result in the form of a map, which relates our stability scenario to the phenomenology of interstellar turbulence: GMC/H I observations, simulations and models.

(iii) GMC turbulence drives the disc to a regime of transition between instability at small scales and stability à la Toomre. Toomre's criterion works instead typically well when applied to discs of cold H I, since the effects of density and velocity fluctuations tend to cancel out. Even so, H I turbulence produces a clear signature in disc morphology. It reduces the characteristic scale of instability by 30–50 per cent or more, depending on the value of Q and on the shape of the energy spectrum. The transition from H I to GMC turbulence occurs when $\Sigma \sim \ell^{1/5}$ and $\sigma \sim \ell^{3/5}$ (for more information, see Section 3).

(iv) Coming astronomical facilities such as Atacama Large Millimeter/submillimeter Array (ALMA)[4] will be able to resolve the scaling properties of galactic turbulence up to very high redshifts. Using our map, such data will show up as *evolutionary tracks*, which will reveal the interplay between gravitational instability and turbulence during the galaxy life. In turn, this will be useful for constraining the sources of galactic turbulence and for understanding the evolution of cosmic star formation.

ACKNOWLEDGMENTS

We are very grateful to John Black, Leo Blitz, Rick Hessman, Ben Moore and Erik Rosolowsky for useful discussions. We are also grateful to an anonymous referee for constructive comments and suggestions. ABR thanks Bruce Elmegreen for strong encouragement and valuable feedback on the occasion of the IAU Symposium 254 'The Galaxy Disk in Cosmological Context'. He also thanks the warm hospitality of both the Department of Physics at the University of Gothenburg and the Department of Fundamental Physics at Chalmers.

REFERENCES

Agertz O., Lake G., Teyssier R., Moore B., Mayer L., Romeo A. B., 2009a, MNRAS, 392, 294
Agertz O., Teyssier R., Moore B., 2009b, MNRAS, 397, L64
Armstrong J. W., Rickett B. J., Spangler S. R., 1995, ApJ, 443, 209
Begum A., Chengalur J. N., Bhardwaj S., 2006, MNRAS, 372, L33
Beresnyak A., Lazarian A., Cho J., 2005, ApJ, 624, L93
Binney J., Tremaine S., 2008, Galactic Dynamics, 2nd edn. Princeton Univ. Press, Princeton, NJ
Bolatto A. D., Leroy A. K., Rosolowsky E., Walter F., Blitz L., 2008, ApJ, 686, 948
Bonazzola S., Falgarone E., Heyvaerts J., Pérault M., Puget J. L., 1987, A&A, 172, 293
Bournaud F., Elmegreen B. G., 2009, ApJ, 694, L158
Burkert A., 2009, in Andersen J., Bland-Hawthorn J., Nordström B., eds, Proc. IAU Symp. 254, The Galaxy Disk in Cosmological Context. Cambridge Univ. Press, Cambridge, p. 437
Chepurnov A., Lazarian A., 2010, ApJ, 710, 853
Dekel A., Sari R., Ceverino D., 2009, ApJ, 703, 785
Dutta P., Begum A., Bharadwaj S., Chengalur J. N., 2008, MNRAS, 384, L34
Dutta P., Begum A., Bharadwaj S., Chengalur J. N., 2009a, MNRAS, 397, L60
Dutta P., Begum A., Bharadwaj S., Chengalur J. N., 2009b, MNRAS, 398, 887

[4] http://www.eso.org/sci/facilities/alma/

Elmegreen B. G., 1996, in Block D. L., Greenberg J. M., eds, New Extragalactic Perspectives in the New South Africa. Kluwer, Dordrecht, p. 467

Elmegreen B. G., 2009, in Andersen J., Bland-Hawthorn J., Nordström B., eds, Proc. IAU Symp. 254, The Galaxy Disk in Cosmological Context. Cambridge Univ. Press, Cambridge, p. 289

Elmegreen B. G., Scalo J., 2004, ARA&A, 42, 211

Elmegreen B. G., Kim S., Staveley-Smith L., 2001, ApJ, 548, 749

Elmegreen D. M., Elmegreen B. G., Ravindranath S., Coe D. A., 2007, ApJ, 658, 763

Fleck R. C., Jr, 1996, ApJ, 458, 739

Förster Schreiber N. M. et al., 2009, ApJ, 706, 1364

Genzel R. et al., 2008, ApJ, 687, 59

Heyer M., Krawczyk C., Duval J., Jackson J. M., 2009, ApJ, 699, 1092

Hughes A. et al., 2010, preprint (arXiv:1004.2094)

Just A., Jacobi S., Deiss B. M., 1994, A&A, 289, 237

Kennicutt R. C. Jr, 1989, ApJ, 344, 685

Kim J., Ryu D., 2005, ApJ, 630, L45

Kim W.-T., Ostriker E. C., 2007, ApJ, 660, 1232

Kim S. et al., 2007, ApJS, 171, 419

Kitsionas S. et al., 2009, A&A, 508, 541

Kowal G., Lazarian A., 2007, ApJ, 666, L69

Kowal G., Lazarian A., Beresnyak A., 2007, ApJ, 658, 423

Kritsuk A. G., Norman M. L., Padoan P., Wagner R., 2007, ApJ, 665, 416

Krumholz M., Burkert A., 2010, preprint (arXiv:1003.4513)

Larson R. B., 1981, MNRAS, 194, 809

Lazarian A., Pogosyan D., 2000, ApJ, 537, 720

Levine R., Gnedin N. Y., Hamilton A. J. S., Kravtsov A. V., 2008, ApJ, 678, 154

McKee C. F., Ostriker E. C., 2007, ARA&A, 45, 565

Martin C. L., Kennicutt R. C. Jr, 2001, ApJ, 555, 301

Padoan P., Jones B. J. T., Nordlund Å. P., 1997, ApJ, 474, 730

Price D. J., Federrath C., 2010, MNRAS, in press (arXiv:1004.1446)

Quirk W. J., 1972, ApJ, 176, L9

Romeo A. B., 1990, PhD thesis, SISSA

Romeo A. B., 1992, MNRAS, 256, 307

Romeo A. B., 1994, A&A, 286, 799

Rosolowsky E., Blitz L., 2005, ApJ, 623, 826

Roy N., Peedikakkandy L., Chengalur J. N., 2008, MNRAS, 387, L18

Schaye J., 2004, ApJ, 609, 667

Schaye J., 2008, in Davies J. I., Disney M. J., eds, Proc. IAU Symp. 244, Dark Galaxies and Lost Baryons. Cambridge Univ. Press, Cambridge, p. 247

Schmidt W., Federrath C., Klessen R., 2008, Phys. Rev. Lett., 101, 194505

Shapiro K. L. et al., 2008, ApJ, 682, 231

Solomon P. M., Rivolo A. R., Barrett J., Yahil A., 1987, ApJ, 319, 730

Tasker E. J., Tan J. C., 2009, ApJ, 700, 358

Toomre A., 1964, ApJ, 139, 1217

Vandervoort P. O., 1970, ApJ, 161, 87

Vázquez-Semadeni E., Gazol A., 1995, A&A, 303, 204

Wada K., Meurer G., Norman C. A., 2002, ApJ, 577, 197

Wadadekar Y., Casertano S., de Mello D., 2006, AJ, 132, 1023

This paper has been typeset from a TEX/LATEX file prepared by the author.